

## Canadian-Based Aircrew Exposure from Cosmic Radiation on Commercial Airline Routes

M.J. McCall, A.R. Green, B.J. Lewis, L.G.I. Bennett, M. Pierre, U. Schrewe\* K. O'Brien† and E. Feldsberger‡

*Royal Military College of Canada, P.O. Box 17000 Stn Forces, Kingston Ontario, Canada K7K 7B4*

*\*Physikalisch Technische Bundesanstalt, Braunschweig, Germany*

*†Northern Arizona University, Flagstaff, Arizona 86011, USA*

*‡University of Graz, Austria*

### Abstract

As part of a continuing study on the occupational exposure of Canadian-based aircrew, a Tissue Equivalent Proportional Counter (TEPC) was used to monitor this exposure on 64 flight routes spanning a range of geomagnetic latitudes between 40°S and 85°N. The microdosimetric data obtained from these flights were compared to that obtained from several terrestrial sources and were used to characterize the radiation field at jet altitudes. From 20 000 ambient dose equivalent rates obtained at various altitudes and geomagnetic latitudes, a correlation was developed to allow for the interpolation of the dose rate for any global position, altitude and date. By integration of this dose rate function over a great circle flight path, a predictive code was developed to provide a total ambient dose equivalent prediction for a given flight.

### Introduction

Recently, it has been determined that jet aircrew are routinely exposed to levels of natural background radiation (i.e., cosmic radiation) which are significantly higher than those present at ground level. In 1990, the International Commission on Radiological Protection (ICRP) recommended that aircrew be classified as occupationally exposed. They also recommended a reduction in the occupational exposure (from 50-20 mSv/yr) as well as a reduction in the general population exposure (from 5 to 1 mSv/yr).<sup>1</sup> In the past, radiation protection regulations did not cover the possibility of overexposure to natural radiation. Recent studies of major Canadian airlines have determined that the exposure to most aircrew is comparable to the average exposures of some nuclear workers.<sup>2</sup> International airline regulators now realize that some type of radiation assessment for aircrew worldwide is most likely to be mandated. This assessment could take several forms, such as the wearing of dosimeters (as in the nuclear industry) or a computer prediction program, based on theory or on an experimental database. If such a program proved successful, the cost and infrastructure of utilizing such a tool would be considerably less than the option of individual monitoring.

This paper describes the method of collecting and analyzing radiation data from numerous worldwide flights, and the encapsulation of results in a program which calculates the radiation dose for any flight in the world at any period in the solar cycle. The use of this experimentally-based program could be used by both the airlines and the (airline) industry regulators.

### Radiation Field Characteristics at Jet Altitudes

The radiation that is found at jet aircraft altitudes (i.e., 20 000 to 45 000 ft) is produced from the interaction of primary high-energy cosmic particles with the nuclei of the Earth's atmosphere. The majority of these primary particles come from outside the solar system and are called galactic cosmic rays (GCR). Primary GCRs consist of ~95% protons and 3.5% alpha particles, with the remainder being

heavy nuclei, typically ranging from carbon to iron.<sup>3</sup> Most of these particles have energies between 100 MeV and 10 GeV.<sup>4</sup> The sun is also a sporadic source of cosmic ray nuclei and electrons that are accelerated by shock waves travelling through the corona, and by magnetic energy released in solar flares. During such occurrences, the intensity of energetic particles in space can increase for hours to days. These solar particle events (SPE) are much more frequent during the active phase of the solar cycle and can reach a maximum energy typically of 10 to 100 MeV, occasionally reaching 1 GeV (roughly once a year) to 10 GeV (roughly once a decade).<sup>5</sup> The effect of GCR to air travellers is generally much greater than the occasional SPE.

The first barrier encountered by the charged GCR as they approach our solar system is the plasma carried by the solar winds (i.e., the solar magnetic field). This solar field acts to decelerate the incoming GCR. When solar sunspot activity is at a maximum (approximately every eleven years), the increased solar field acts to screen out low-energy galactic particles that would otherwise enter into the solar system. Thus, cosmic ray intensities also vary in a cyclical pattern, but in a manner anticoincident with solar activity. This fluctuation in GCR abundance is measured by neutron monitors on Earth and is converted to a parameter called heliocentric potential,  $U$ , which is directly related to a point in the solar cycle.<sup>6</sup>

The GCRs which are not deflected by the solar magnetic field now encounter the Earth's magnetic field. The success of these particles to penetrate or diffuse through the magnetic field is dependent on their angle of incidence and its magnetic rigidity,  $R_p$ , which is related to its momentum and charge, i.e.,

$$R_p = \frac{pc}{q} \quad [1]$$

where  $p$  is the particle's momentum,  $q$  is the particle charge of the particle and  $c$  is the speed of light.<sup>7</sup> A particle can enter the Earth's atmosphere if its magnetic rigidity,  $R_p$ , is greater than the vertical cutoff rigidity of the Earth's magnetic field,  $R_c$ , at its point of entry. The vertical cutoff rigidity (in GV) is related to the geomagnetic latitude,  $B_m$ , (in radians) by the Störmer equation:<sup>8</sup>

$$R_c = \frac{14.9 \cos^4 B_m}{r_e^2} \quad [2]$$

where  $r_e$  is given in Earth radii. The geomagnetic latitude,  $B_m$ , is calculated from the geographic latitude and longitude ( $\lambda, \phi$ ) according to:<sup>9</sup>

$$\sin B_m = \sin \lambda \sin \lambda_p + \cos \lambda \cos \lambda_p \cos (\phi - \phi_p) \quad [3]$$

where  $\lambda_p=79.3^\circ\text{N}$  and  $\phi_p=289.89^\circ\text{E}$  (the position of the geomagnetic north pole). This penetrating ability of GCRs has been measured experimentally by Shea et al. and the results are shown in [Figure 1](#), with  $R_c$  plotted as global contours. Effectively, the higher the  $R_c$  value, the fewer the number of GCRs that are able to penetrate into the atmosphere at a given global position. At the equator, the cutoff rigidity is highest as the magnetic field shape is horizontal to the Earth and reflects vertically incident GCRs with a rigidity,  $R_p$ , of less than 16 GV. At the poles, the field is almost vertical and the cutoff rigidity is almost zero, allowing the maximum number of GCRs to penetrate. At jet aircraft altitudes during a solar minimum (i.e., when galactic radiation is at a maximum), GCR radiation is 2.5-5 times more intense at the poles than at the equatorial regions.<sup>10</sup> The cutoff rigidity curve displays another interesting feature, the so called "geomagnetic knee", which is a fairly large region above approximately  $50^\circ\text{N}$  in Canada or  $70^\circ\text{N}$  in Siberia where the radiation levels are constant with increasing latitude.

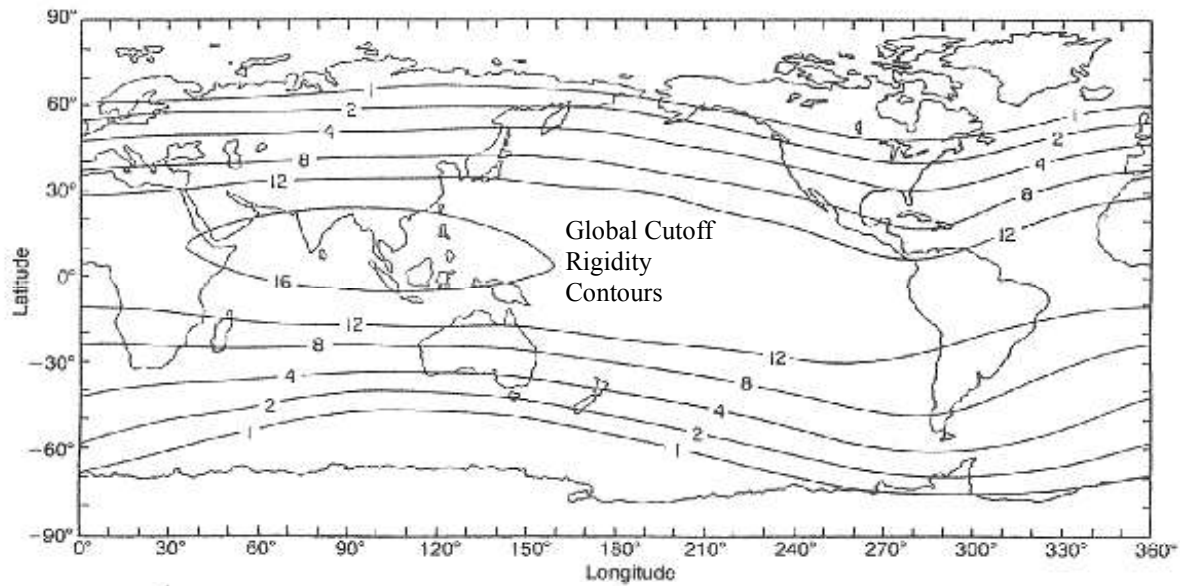


**Figure 1** Global vertical cutoff rigidity values. (Taken from reference 10)

With penetration of the Earth's magnetic field, the GCRs are subjected to yet another natural shield, the atmosphere of the Earth. These primary cosmic particles collide with atmospheric nitrogen and oxygen nuclei producing secondary particles that include neutrons, protons and pions (which quickly decay to produce muons, neutrinos and gamma rays), as well as electrons and positrons produced by muon decay and gamma ray interactions with atmospheric atoms.<sup>11</sup> The buildup of these secondary particles competes with their reduction through energy loss and further interactions with other atmospheric nuclei. This results in dose rates which vary with altitude, reaching a maximum level at 20 km above sea level, known as the Pfozter maximum.

### Experimental Procedure

Since radiation effects vary with altitude, geomagnetic latitude and heliocentric potential (as indicated above), the primary goal of this research was to obtain data that were valid for this complex spectrum present at aircraft altitudes. The data collected must cover the full range of the altitude, latitude and heliocentric potential parameters to allow for the development of a global model for flight dose prediction. The measurement instrument had to be portable, simple to operate and battery powered to allow it to fly on any aircraft without the presence of research personnel.

The best instrument for this complex-field measurement is a Tissue Equivalent Proportional Counter (TEPC). It provides not only an indication of the total dose equivalent, but also the microdosimetric distribution of the radiation as a function of linear energy transfer (LET). The 5"-diameter TEPC used in this study was designed by Battelle, Pacific Northwest National Laboratories to be an extremely portable instrument. It fits into any overhead bin and is powered by batteries which last up to five days of operation. It is simple to operate (off/on switch only) and stores a microdosimetric spectrum every minute for up to thirty days of operation. The stored binary data can be downloaded to any computer and proprietary software can produce an output of absorbed dose,  $D$ , and dose equivalent,

$H$ , versus time. In addition to these outputs, the raw spectral TEPC data can be output as a microdosimetric dose distribution that can provide an estimate of the average quality factor,  $\bar{Q}$ , of the radiation field of interest.

As described in previous works,<sup>12</sup> the TEPC was calibrated initially by the manufacturer using <sup>137</sup>Cs and <sup>252</sup>Cf sources. This calibration was checked routinely with an internal <sup>244</sup>Cm source, which, in normal operation, is shielded from the detector cavity by a magnetic shutter. Since the radiation field at jet altitudes is so complex, the response of the TEPC was verified in several types of terrestrial radiation fields prior to use at jet altitudes. Measurements of the cosmic radiation field were made on board 64 flights worldwide, covering an altitude range up to 42 000 feet and a range of geomagnetic latitudes from 80°N to 45°S (equivalent to a full range of  $R_c$ ). For the majority of the in-flight measurements, aircrew turned on the TEPC prior to takeoff and off after landing and provided positional data consisting of the flight course and altitude history. Since the TEPC has its own internal clock, the TEPC measurements could then be correlated to the plane's position (geomagnetic latitude and altitude) at one-minute intervals.

### Microdosimetry Theory

The TEPC monitors radiation by detecting the electrical signal that results from the ionization of the detector gas (propane) following an energy-deposition event. The pulse size of this signal is directly proportional to the number of ion pairs formed, and hence proportional to the energy imparted,  $\epsilon$ , and is linearly amplified in magnitude by gas multiplication. Because the dynamic range of these pulses is often very large (e.g., over 5 orders of magnitude for fast neutrons), the spectrum of energy imparted is measured in two different sections, differing in gas gain level, and hence in resolution, from each other. The signals received from the detector are sorted by a MCA into 256 channels according to pulse height so that the final output from the TEPC is the number of counts,  $n$ , as a function of channel number in each of the two different gain regions. The channel number is related to the lineal energy,  $y$  (which is the quotient of the energy imparted in a given volume by a single energy-deposition event to the mean chord length of the volume) such that each channel has a bin width of 0.1 keV/ $\mu$ m in the high-gain region and a bin width of 5 keV/ $\mu$ m in the low-gain region. The two overlapping segments are joined to produce an event frequency distribution. A detailed description of the treatment of this frequency distribution is given in Reference 2; however, the pertinent equations are summarized below.

In order to compare spectra measured under different conditions, it is necessary to normalize the frequency distribution so that the total area under the curve represents one event.<sup>13</sup> This can be accomplished by utilizing the probability density function  $f(y)$  (also called the lineal energy distribution), which is defined as

$$f(y) = \frac{dF(y)}{dy} \approx \frac{\Delta F(y_i)}{\Delta y_i} \equiv f(y_i) = \frac{n(y_i)}{\Delta y_i \sum_{i=0}^{\infty} n(y_i)}, \quad [4]$$

where  $F(y)$  is the probability that the lineal energy is equal to or less than  $y$  and  $\Delta y_i$  is the appropriate bin width as described above. Note that this function satisfies the normalization condition of any probability density function, i.e.,

$$\int_0^{\infty} f(y) dy = 1. \quad [5]$$

The frequency-mean lineal energy,  $\bar{y}_F$ , is the expectation value of  $y$  (i.e., the average of the observed values of  $y$ ), as weighted by the frequency probability density, i.e.,

$$\bar{y}_F = \frac{\int_0^{\infty} yf(y)dy}{\int_0^{\infty} f(y)dy} = \int_0^{\infty} yf(y)dy \approx \sum_{i=0}^{\infty} y_i f(y_i) \Delta y_i = \frac{\sum_{i=0}^{\infty} y_i n(y_i)}{\sum_{i=0}^{\infty} n(y_i)}. \quad [6]$$

It is often more useful to consider the dose distribution of  $y$  (as opposed to the frequency distribution). The dose probability density,  $d(y)$ , can be related to  $f(y)$  and  $\bar{y}_F$  by:

$$d(y) = \frac{1}{\bar{y}_F} yf(y). \quad [7]$$

Note that  $d(y)$  is also a normalized probability density function. Analogous to  $\bar{y}_F$ , the dose-mean lineal energy,  $\bar{y}_D$ , is an expectation value of  $y$  weighted with the dose probability density, i.e.,

$$\bar{y}_D = \int_0^{\infty} yd(y)dy. \quad [8]$$

Since the values of both  $y$  and  $d(y)$  can range over several orders of magnitude, a linear representation will not show the details of the distribution. For this reason, the dose distribution is normally plotted in a semi-logarithmic representation as  $yd(y)$  versus  $\log y$ . In this representation, the area under the curve in a given  $y$  interval is proportional to the fraction of *dose* delivered by events with lineal energies in this interval.

Similarly, a *dose equivalent* probability density function can be calculated using  $h(y)=d(y)q(y)$ , where  $q(y)$  is the quality factor relationship taken from the ICRU Publication 40.<sup>14</sup> Alternatively,  $y$  can be equated to the *LET* so that  $q(y)$  can be replaced by the  $Q(LET)$  relationship given in ICRP-60, which results in only a 3% decrease in the integrated dose equivalent.<sup>2</sup>

The absorbed dose,  $D$  (in Gy), and the dose equivalent,  $H$  (in Sv), for a given event frequency distribution (i.e., spectrum) can be further calculated as follows:

$$D = \frac{0.204}{d_d^2} \sum_{i=0}^{\infty} y_i n(y_i) \quad [9]$$

$$H = \frac{0.204}{d_d^2} \sum_{i=0}^{\infty} q(y_i) y_i n(y_i) \quad [10]$$

where, for the current detector,  $d_d = 1.27 \times 10^5 \mu\text{m}$  and the  $Q(LET)$  (i.e., the ICRP-60 relation) is adopted for  $q(y)$  in the present analysis. The average quality factor is further given by:

$$\bar{Q} = \frac{H}{D} = \int_0^{\infty} q(y)d(y)dy. \quad [11]$$

## Microdosimetric Field Measurements

### Ground-Based Measurements

As part of a continuing assessment of the cosmic radiation exposure of Canadian-based aircrew, the TEPC was used to take dosimetric measurements on board 64 flights from September 1998 to October 1999. In conjunction with these in-flight measurements, the operation of the TEPC was verified using several common radioisotopic sources, such as  $^{137}\text{Cs}$ ,  $^{60}\text{Co}$ ,  $^{252}\text{Cf}$ ,  $^{241}\text{Am}$ - $^9\text{Be}$  and  $^{239}\text{Pu}$ - $^9\text{Be}$ .<sup>12</sup> The individual microdosimetric spectra recorded by the TEPC in each of these fields represent the different constituents present in the radiation field at high altitudes (i.e., the gamma and neutron components of the field) as shown in Reference 12. The high-LET (i.e., neutron) component of the radiation field created by cosmic rays at jet altitudes can be simulated on the ground by the radiation field produced behind concrete shielding at accelerator facilities. The CERN/European Commission high-energy reference field facility (CERF) has been used for this purpose since 1993.<sup>15</sup> This facility is set up at one of the secondary beams from the Super Proton Synchrotron at CERN. The particles (protons and pions) from a charged hadron beam hit a copper target, 50 cm thick and 7 cm in diameter. The secondary particles resulting from this interaction are then filtered by an 80-cm thick concrete shielding placed above the copper target. The microdosimetric spectrum recorded by the TEPC on top of this shielding is shown compared to an in-flight microdosimetric spectrum in Figure 2. Although the shape of the high-LET ( $> 10 \text{ keV}/\mu\text{m}$ ) portion is similar in both spectra (as expected from the similarities in the neutron spectra); the relative area represented by the high-LET portion of each spectrum is significantly different. This difference is a direct result of the difference in the relative proportion of neutrons in each field. At the CERF field intensity represented in Figure 2A, neutrons contribute about 85% of the total dose equivalent, compared to approximately 50% at jet altitudes. As a result, the relative area under the curve for  $y > 10 \text{ keV}/\mu\text{m}$  is much greater in the CERF spectrum (Figure 2A) than in the jet-altitude spectrum (Figure 2B). In addition, the low-LET portion of the spectrum obtained at CERF is dominated by a background muon contribution which is not present at jet altitudes.

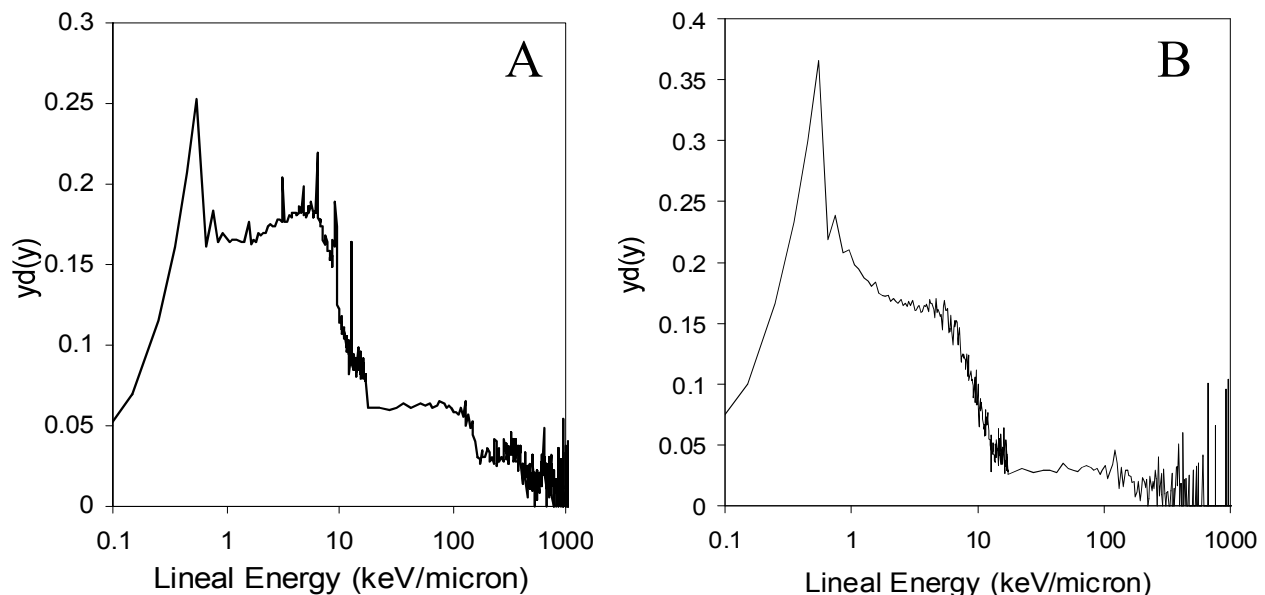


**Figure 2** Comparison of microdosimetric dose distributions obtained (A) on top of the concrete shielding at CERF at a field intensity of 3500 Precision Ion Chamber (PIC) counts per pulse (summed over 3 hours) and (B) on a 8 hour flight between Zurich and Toronto at an altitude of 37 000 feet.

**Table 1** Microdosimetric Quantities Obtained from Ground-Based Sources

Source	Type of Radiation	$\bar{y}_F$ (keV/ $\mu\text{m}$ ) <sup>a</sup>	$\bar{y}_D$ (keV/ $\mu\text{m}$ )	$\bar{Q}$
<sup>137</sup> Cs	$\gamma$ rays	$0.36 \pm 0.13$	$7.2 \pm 0.8$	$1.1 \pm 0.2$
CERF	neutrons, muons, $\gamma$ rays	0.50	$30 \pm 3$	$3.8 \pm 0.7$
<sup>239</sup> Pu- <sup>9</sup> Be	neutrons, $\gamma$ rays	1.39	$51 \pm 6$	$9 \pm 2$
<sup>244</sup> Cm	$\alpha$ particles	14.0	$150 \pm 20$	$24 \pm 4$

<sup>a</sup>The maximum error on  $\bar{y}_F$  is 35%, most of which is associated with the extrapolation to zero lineal energy; thus, this error will be most significant for gamma ray spectra.

The values of the microdosimetric quantities of  $\bar{y}_F$ ,  $\bar{y}_D$  and  $\bar{Q}$  obtained from several terrestrial sources, including those obtained from the CERF spectrum in Figure 2A, are shown in Table 1. The quantity  $\bar{y}_F$  gives the average lineal energy per event; however, the quantities  $\bar{y}_D$  and  $\bar{Q}$  are more useful in radiation protection since they are more representative of the relative biological effectiveness (RBE) of the measured radiation. In particular,  $\bar{Q}$  should provide an approximation of the radiation weighting factor,  $w_R$ , as defined in ICRP-60.<sup>1</sup> For instance, the experimental  $\bar{Q}$  value of 1.1 obtained for gamma rays from a <sup>137</sup>Cs source agrees quite well with the  $w_R$  value of 1 recommended in ICRP-60. As expected, fields with more biologically-damaging particles (such as the <sup>239</sup>Pu-<sup>9</sup>Be neutron field) will have higher values of  $\bar{Q}$  and  $\bar{y}_D$ . The values of these quantities obtained from terrestrial sources can provide a useful comparison to the values obtained from the radiation field at jet altitudes.

Finally, before using the TEPC to monitor radiation at jet altitudes, it is necessary to know the response of the TEPC relative to the ambient dose equivalent,  $H^*(10)$ . In other words, the TEPC must be calibrated in a known neutron field to obtain a multiplication factor,  $f$ , which can be applied to  $H_{TEPC}$  such that:<sup>16</sup>

$$H^*(10) = f H_{TEPC}. \quad [12]$$

The response of the TEPC was compared to  $H^*(10)$  in polyenergetic neutron reference fields (<sup>252</sup>Cf and AmBe) and in monoenergetic neutron beams at the Physikalisch Technische Bundesanstalt (PTB). The results from the polyenergetic neutron fields are shown in Table 2, while the results from the monoenergetic neutron beam measurements are shown in Figure 3.

**Table 2** Response of RMC TEPC to Polyenergetic Neutron Reference Fields

Source	Reference ( $H^*(10)$ ) Dose Rate [ $\mu\text{Sv/hr}$ ]	Measured Dose Rate <sup>a,b</sup> [ $\mu\text{Sv/hr}$ ]	Relative Difference [%]
<sup>252</sup> Cf	996 +/- 24	1165	16.9
Am(Be)	11.8 +/- 0.6	14.2	20.6

<sup>a</sup>For  $y > 10$  keV/ $\mu\text{m}$  (neutrons only).

<sup>b</sup>Corrected for backscattering (using shadow cone).

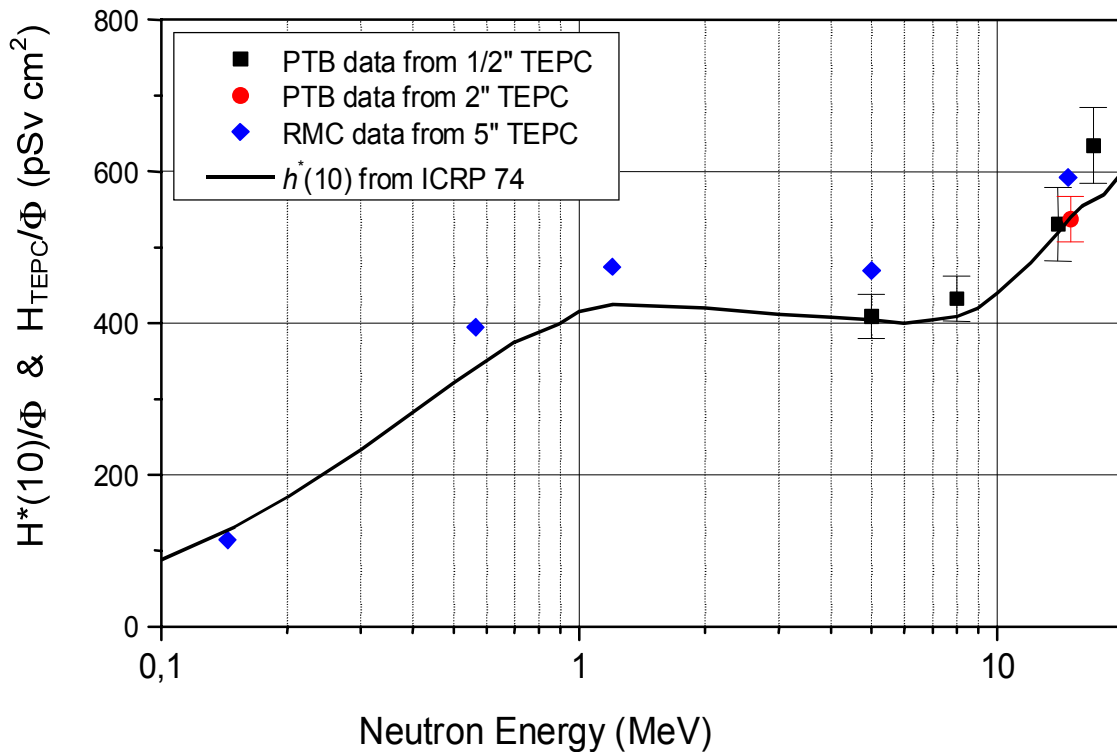


**Figure 3** Response of RMC TEPC compared to  $H^*(10)/\Phi$  at selected neutron energies. The response of the RMC TEPC,  $H_{TEPC}/\Phi$  (blue diamonds), is compared to  $H^*(10)/\Phi$  values given in ICRP-74 (solid line). Responses of PTB-owned TEPC's are also shown for comparison (black and red symbols). Graph compliments of U. Schrewe of PTB.

These measurements show that  $H_{TEPC}$  is systematically higher than  $H^*(10)$  (by an average of ~15%, excluding the measurement at a neutron energy of 0.144 keV, where the TEPC is known to under-respond since the range of the recoil proton is less than the TEPC diameter). In addition, comparison to a calibrated  $^{137}\text{Cs}$  gamma source shows that the TEPC over-responds to gamma rays by approximately 10%. Based on these results,  $f$  in Equation 12 should be  $1/1.15 = 0.870$ .

#### *At-Altitude Measurements*

Microdosimetric spectra were obtained on board 64 worldwide flights flown at altitudes between 15 000 and 41 000 feet. A typical dose distribution for a trans-Atlantic flight is shown in [Figure 2B](#). For a portion of these flights at altitudes greater than 28 000 feet, values of  $\bar{y}_F$ ,  $\bar{y}_D$  and  $\bar{Q}$  were obtained from TEPC spectral data summed over an entire flight (Table 3). The values of all three of these quantities are all very similar to those obtained from the radiation field on top of the shielding at CERF. On all flights, the  $\bar{Q}$  values are greater than 1 and the  $\bar{y}_D$  values are greater than 10 keV/ $\mu\text{m}$ , which indicates a significant high-LET (> 10 keV/ $\mu\text{m}$ ) contribution to the radiation field. In particular, the values of both of these quantities are higher than those from radiation fields experienced by terrestrial radiation workers (where  $Q \sim 1$ ). This indicates that aircrew are exposed to a radiation field which has a higher deposition density (LET), for which there is a greater uncertainty in the biological risk coefficient.

**Table 3** Microdosimetric Quantities Measured on Canadian-based Flights

Global Flight Region	Routes Covered <sup>a</sup>	$\bar{y}_F$ (keV/ $\mu$ m)	$\bar{y}_D$ (keV/ $\mu$ m)	$\bar{Q}$
Trans-Atlantic	YYZ-LHR (return)	0.358	14 $\pm$ 2	2.3 $\pm$ 0.4
	YYZ-FRA (return)			
	YYZ-ZRH (return)			
	YUL-LHR LHR-YVR			
Trans-Canada	YYZ-YVR (2)	0.359	15 $\pm$ 2	2.3 $\pm$ 0.4
	YVR-YYZ (3)			
Caribbean	YYZ-BGI	0.340	13 $\pm$ 2	2.2 $\pm$ 0.4
	BGI-YYZ			
Trans-Pacific	YVR-KIX	0.334	15 $\pm$ 2	2.2 $\pm$ 0.4
	KIX-YVR			

<sup>a</sup>Airport codes are YYZ-Toronto International; LHR-Heathrow, London, UK; FRA-Frankfurt, Germany; ZRH-Zurich, Switzerland; YUL-Dorval, Montreal; YVR-Vancouver; BGI-Bridgetown, Barbados; KIX-Osaka, Japan

### Model Development for Route-Dose Prediction

In addition to these microdosimetric quantities, the raw TEPC output can also be manipulated to give the quantities of absorbed dose,  $D$ , and dose equivalent,  $H$ , (see Equations 9 and 10). These quantities were obtained by summing the spectral data over five-minute intervals. Data smoothing was applied using a least squares method developed by Savitzky and Golay<sup>17</sup> to reduce the relative error on the data to approximately 15%. This method of data treatment was applied to the TEPC spectral data obtained from 36 flights (a training sub-set of the original 64 flights). This resulted in over 20 000 dose equivalent rate data points which are plotted as a function of altitude and geomagnetic latitude in [Figure 4](#). This figure shows a consistent symmetry between altitude curves, which is due to the shielding effect of the atmosphere. If the dose equivalent rate data are plotted logarithmically as a function of the atmospheric depth, a linear relationship is expected in accordance with radiation shielding theory, in which the slope of the resulting line is simply the mass attenuation coefficient of the atmosphere,  $\mu/\rho$ . This result is depicted in [Figure 5](#), where the original data are plotted for different geomagnetic positions of 0, -30, 30, 45, 60, 75 and 90 degrees. An average slope of the resulting lines yields a value of  $\mu/\rho = 0.0062 \text{ cm}^2/\text{g}$  which is in excellent agreement with a literature value of  $0.0063 \text{ cm}^2/\text{g}$ .<sup>18</sup>

This mass attenuation coefficient for the atmosphere (valid over the altitudes 31 000 to 39 000 feet) can be used to normalize the data in [Figure 4](#) to a specific altitude. In particular, the dose rate at 35 000 ft (i.e.,  $h_o = 243 \text{ g/cm}^2$ ) can be derived from the dose rate at any depth  $h$  according to:

$$\dot{H}(h) = \dot{H}_o e^{-(\mu/\rho)(h - h_o)} \quad [13]$$

Normalizing all data from various altitudes to 35000 feet in this manner yields [Figure 6](#).

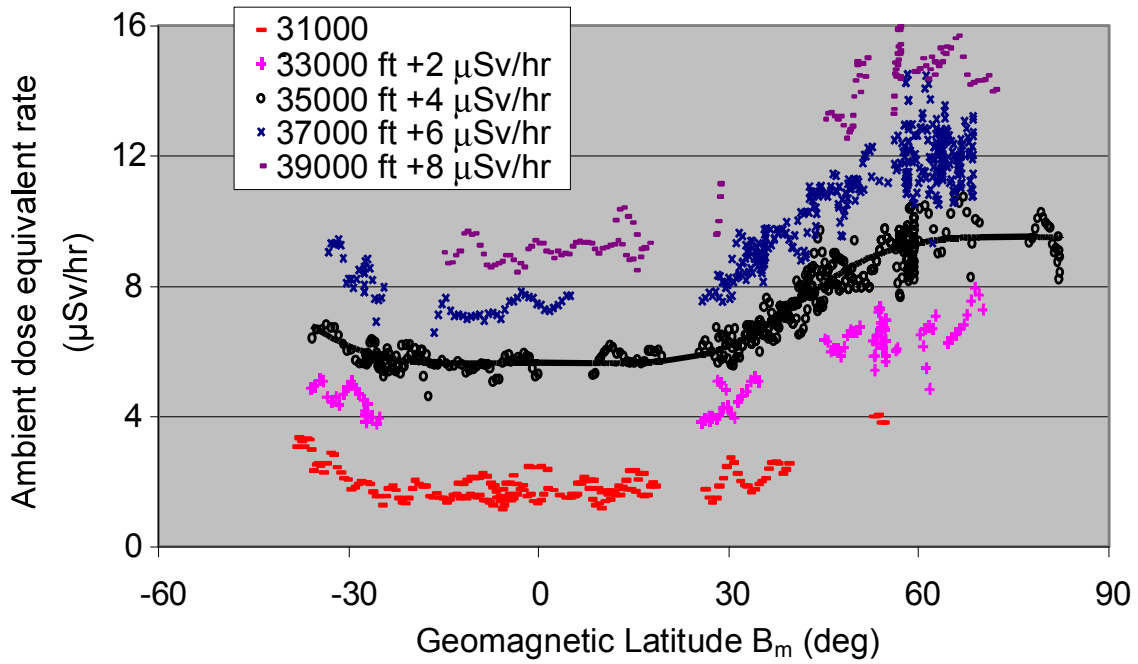


**Figure 4** Experimental dose rate data versus geomagnetic latitude for various altitudes. (The curves are displaced for improved clarity by the values given in the figure).

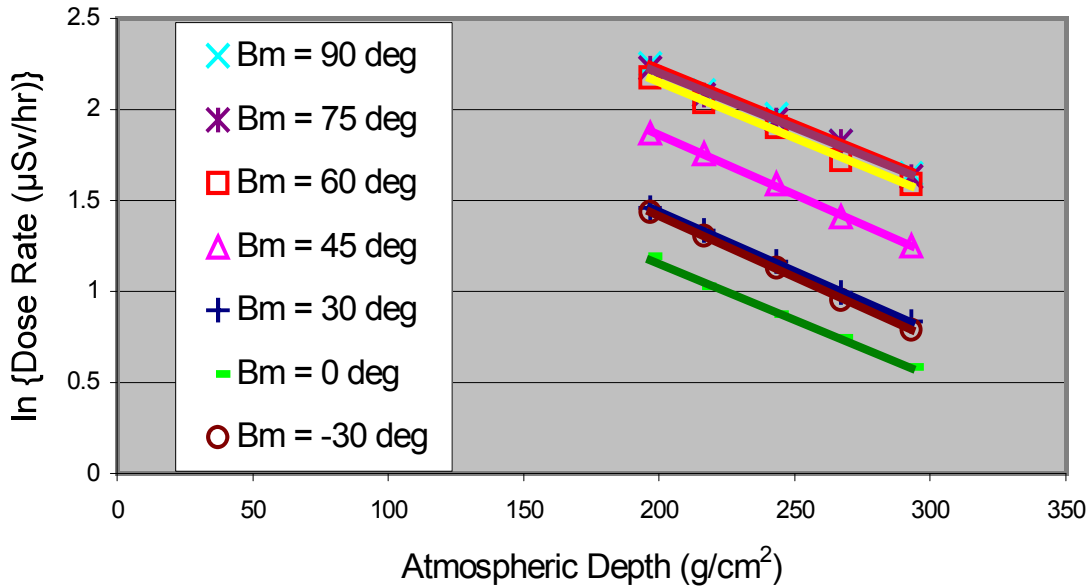


**Figure 5** Plot of  $\ln(\dot{H})$  versus atmospheric depth at various global positions.

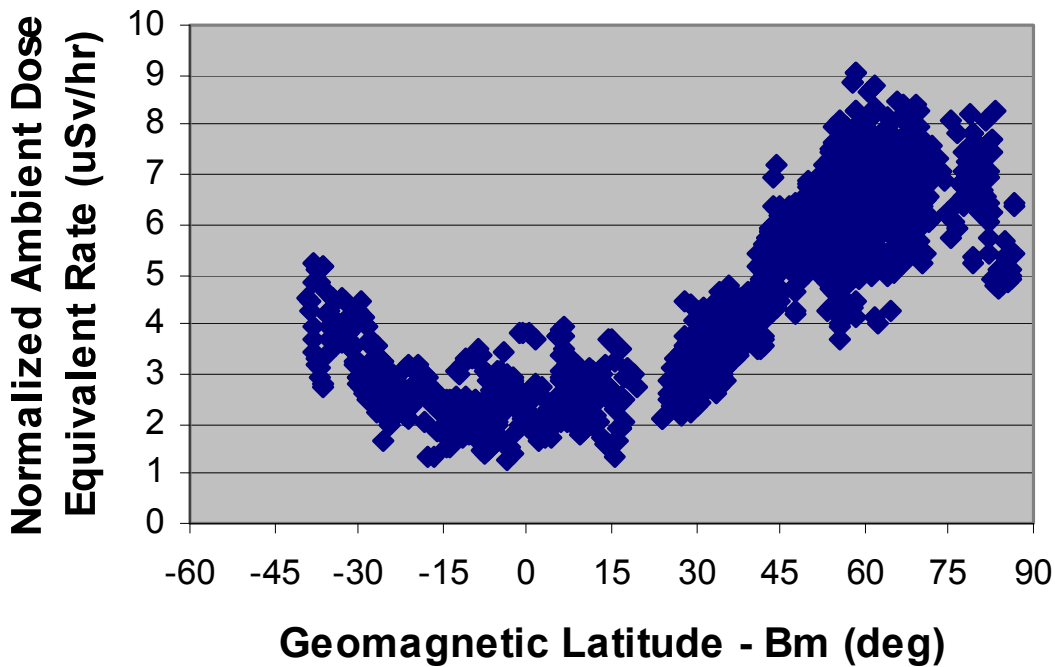


**Figure 6** Dose rate (normalized to 35000 feet) versus geomagnetic latitude.

To account for solar cycle effects, a normalizing function for heliocentric potential was found using the CARI 5E transport code. About 1350 CARI 5E runs were compiled, for 23 flights worldwide at six-month intervals over a 28-year period and at 35 000 feet. The effective dose of each flight was normalized to a heliocentric potential of 650 MV. A best fit line was used to allow for interpolation of  $U$  for values from 400 to 1500 MV, where

$$f(U) = -0.000271U + 1.181 \quad [14]$$

and  $f$  is normalized to a value of unity at 650 MV.

On further examination of the symmetry around the equator in [Figure 6](#) (with a mirroring of data), it was seen that the north to south symmetry was not exact. This is due in part to the 10.7° offset of the spin axis of the Earth with respect to the magnetic dipole axis which gives rise to deviations in the magnetic field. As well the data collected do not span the full range of geomagnetic coordinates, which limits the ability of the correlation as a reliable method for interpolating the dose rate for any flight worldwide. To allow for the asymmetries of the earth's magnetic field, the data can be plotted instead as a function of the vertical cutoff rigidity ([Figure 7](#)).

[Figure 7](#) shows that the experimental data collected on the training set flights cover all possible values of vertical cutoff rigidity ( $R_c$ ) from 0-16 GV. A correlation of the global dose rate as a function of  $R_c$  is therefore possible for a given global position (i.e., geomagnetic latitude ( $B_m$ )). Symmetry was verified by differentiating data collected north of the equator with that south of the equator. The two sets of data overlapped, showing that the relationship of dose rate and  $R_c$  (within experimental uncertainties) is symmetric around the equator and is in fact a better representation than a plot of dose equivalent rate versus  $B_m$ . The final step was the development of a best-fit polynomial to the data in [Figure 7](#). This equation is used for the code development to allow for dose rate prediction for any global position (with corrections for altitude effects using Equation 13 and solar cycle effects using Equation 14).

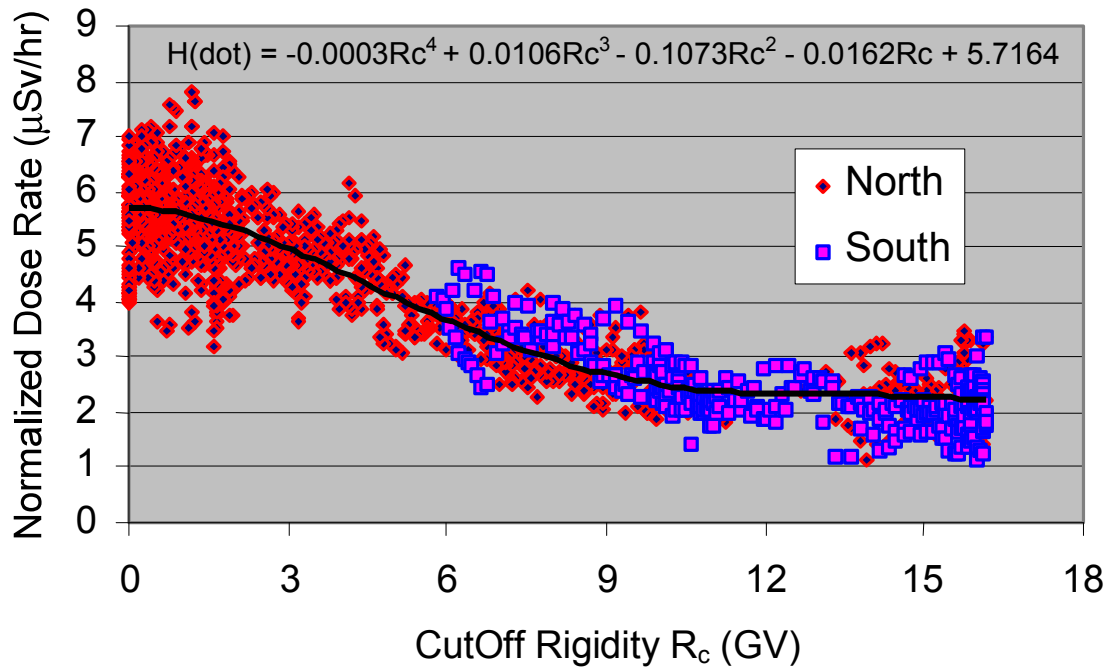


**Figure 7** Plot of dose rate (normalized to U = 650 MV and 35 000 feet) versus effective vertical cutoff rigidity,  $R_c$  (GV).

### Comparison to Other Work

The Physikalisch Technische Bundesanstalt (PTB) in Braunschweig, Germany have conducted concurrent research very similar to that described in this paper. In the PTB analysis measurements with a neutron monitor and an ion chamber were summed to produce a total dose equivalent rate. The instrumentation was flown on 39 flights worldwide.<sup>19</sup> The PTB data were forwarded to RMC for comparison. These data were normalized to 35000 feet and 650 MV using the methods described for the RMC data. These data were compared in a plot of dose equivalent rate versus  $R_c$ , with agreement within 5% (Figure 8). The RMC data were also compared to predictions with the LUIIN 2000 transport code which simulated the RMC flights for a constant altitude of 35 000 feet and 650 MV (Figure 8). There is excellent correlation between experimental and theoretical ( $H^*10$ ) values, which are within 7%. The LUIIN 2000 curve is practically identical to the best-fit polynomial of the RMC data in Figure 7.

### Code Development and Validation

The computer program PC-AIRE was developed, in a Visual C++ platform, from the data analysis and the equations produced therein. This code was written to be user-friendly and requires minimal time for data input, calculation and data storage. The code requires the user to input the date of the flight, the origin and destination airports, the altitudes and times flown at those altitudes. Look-up tables produce the latitude and longitudes of origin and destination, as well as the heliocentric potential. A great circle route is produced between the two airports, and the latitude and longitude of that great circle are calculated for every minute of the flight.<sup>20</sup> The effective cutoff rigidity is either calculated from Equations 2 and 3 or interpolated from tabulated data for the given geographical coordinates along the flight path. The dose rate is then integrated along the great circle path at one minute intervals (using the correlation in Figure 7), and unfolded to the actual altitude flown (Equation 13) and heliocentric potential

value (Equation 14). The code outputs the total ambient dose equivalent for the flight. PC-AIRE was validated against the remaining 28 flights from the original experimental set collected with the RMC TEPC (i.e., the validation set). As shown in Figure 9, the PC-AIRE predictions of the validation flights are in very good agreement with the TEPC measurements for those flights.

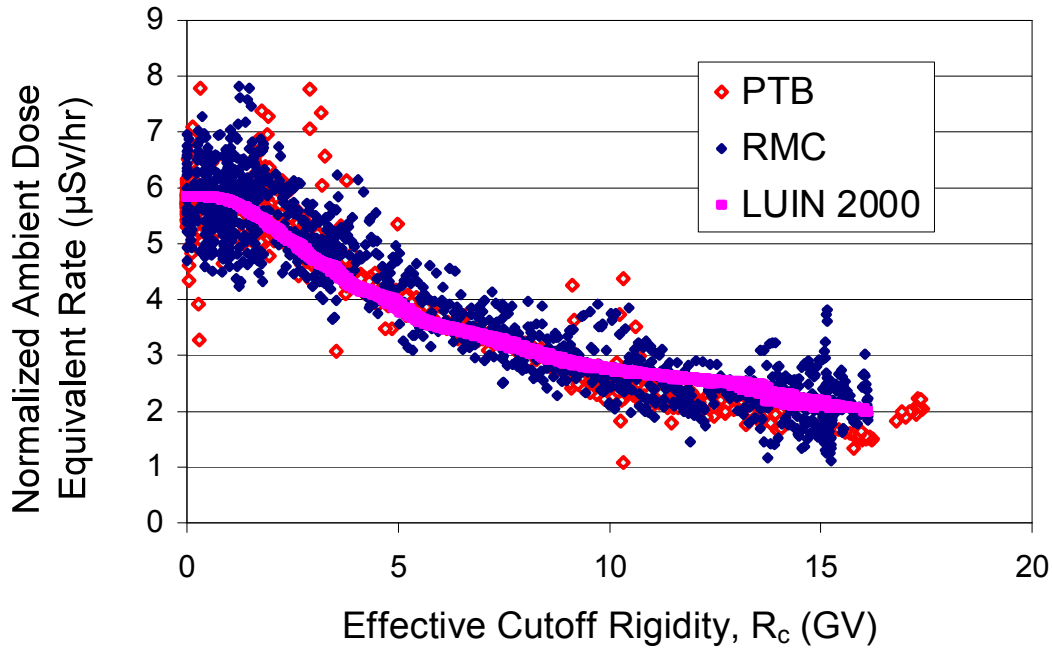


**Figure 8** Comparison of the experimental data at RMC and PTB (normalized to  $U=650$  MV and 35000 feet) with the LUIN 2000 code predictions.

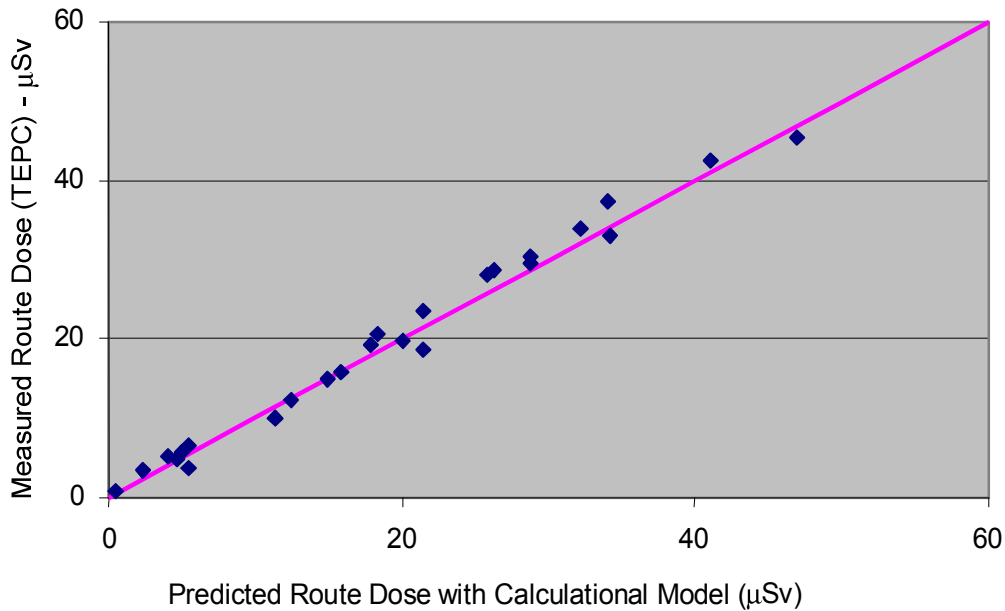


**Figure 9** Plot of PC-AIRE Predicted Flight Dose- $H^*10$  ( $\mu\text{Sv}$ ) versus TEPC measured results.

## Conclusions

Twenty thousand TEPC data points were collected on 64 flights spanning the globe. These data were analyzed to produce a semi-empirical model for global prediction of flight dose which accounts for the effects of altitude, latitude and solar cycle. This model was utilized in a predictive code, PC-AIRE, which considered an integration of the dose rate along a great-circle path. The code was subsequently validated using additional experimental data collected with a TEPC. The code has proven to be simple to operate with results in excellent agreement with other experimental data collected by PTB and theoretical results from a transport code developed in the United States. This code is the first program in the world to predict total flight dose, based on experimental data obtained from actual worldwide flights.

## Acknowledgements

The authors would like to thank J. Servant of Transport Canada and S. Kupca and C. Thorp of the Director General Nuclear Safety (DGNS) of the Department of National Defence for their assistance in this study. The authors would also like to express their gratitude to the employees and management of Air Canada, First Air and British Airways for their assistance and cooperation in the arrangement for measurements on board commercial flights. In particular, the authors wish to thank J. Nakielny, C.J. Saint-Martin and C. Thibeault of Air Canada, J. Lafrance of First Air and D. Irvine of British Airways. The authors would also like to thank 1 Canadian Air Division of the Canadian Forces, Air Operations at 8 Wing Trenton and the crewmembers of 437, 436 and 429 Squadrons for their cooperation and assistance in data collection on board military flights. The authors wish to thank Dr. M. Silari and A. Mitaroff at CERF for their considerable time and efforts and also Dr. H. Bonin of RMC for useful discussions. Financial support for this study was received from Transport Canada Commercial and Business Aviation Division and DGNS.

## References

1. International Commission on Radiological Protection, *1990 Recommendations of the International Commission on Radiological Protection*, ICRP Publication 60, Pergamon Press, Oxford (1991).
2. B.J. Lewis, P. Tume, L.G.I. Bennett, M. Pierre, A.R. Green, T. Cousins, B.E. Hoffarth, T.A. Jones and J.R. Brisson, *Cosmic Radiation Exposure on Canadian-Based Commercial Airline Routes*, *Radiat. Prot. Dosim* **86**(1), 7-24 (1999).
3. K. O'Brien, W. Friedberg, H.S. Sauer and D.F. Smart, *Atmospheric Cosmic Rays and Solar Energetic Particles at Aircraft Altitudes*, *Environ. Int.* **22**, (Suppl. 1), S9-S44 (1996).
4. T.K. Gaisser, *Cosmic Rays and Particle Physics*, Cambridge, Cambridge University Press (1990).
5. J.A. Simpson, *Elemental and Isotopic Composition of the Galactic Cosmic Rays*, *Ann. Rev. Nucl. Part. Sci.*, **33**, 323-381 (1983).
6. P. Goldhagen, *Overview of Aircraft Radiation Exposure and Recent ER-2 Measurements*, Submitted to NCRP Proceedings No. 20, *Cosmic Radiation Exposure of Airline Crews, Passengers and Astronauts*, New York, N.Y. (1999).
7. S. Hayakawa, *Cosmic Ray Physics: Nuclear and Astrophysical Aspects*, Wiley and Sons, New York, (1969).

8. M.A. Shea, D.F. Smart and L.C. Gentile, *Estimating Cosmic Ray Vertical Cutoff Rigidities as a Function of the McIlwain L-parameter for Different Epochs of the Geomagnetic Field*, *Physics of the Earth and Planetary Interiors* **48**, 200-205 (1987).
9. T.F. Tascione, *Introduction to the Space Environment*, Orbit Book Company, Malabar, Florida (1988).
10. G. Reitz, *Radiation Environment in the Stratosphere*, *Radiat. Prot. Dosim.* **48** (1), 5-20 (1993).
11. K. O'Brien and J.E. McLaughlin, *The Radiation Dose to Man from Galactic Cosmic Rays*, *Health Physics*, **22**, 225-232 (1972).
12. A.R. Green, B.J. Lewis, L.G.I. Bennett, M. Pierre and T. Cousins, *Commercial Aircrew Radiation Dosimetry using a Tissue Equivalent Proportional Counter*, In Proceedings of the 20<sup>th</sup> Annual Conference of the Canadian Nuclear Society, Montreal, Quebec, 30 May – 2 June 1999.
13. A.J. Waker, *Principles of Experimental Microdosimetry*, *Radiat. Prot. Dosim.*, **61**, 297-308 (1995).
14. International Commission on Radiation Units and Measurements, *The Quality Factor in Radiation Protection*, ICRU Publication 40, April 1986.
15. C. Birattari, T. Rancati, A. Ferrari, M. Hofert, T. Otto and M. Silari, *Recent Results at the CERN-EC High Energy Reference Field Facility*, In Proceedings of the Third Specialists Meeting on Shielding Aspects of Accelerators, Targets and Irradiation Facilities, Tohoku University, Sendai, Japan 12-13 May 1997, pp. 219-234.
16. J.C. Nunes, A.J. Waker and A. Arneja, *Neutron Spectrometry and Dosimetry in Specific Locations at Two CANDU<sup>®</sup> Power Plants*, *Radiat. Prot. Dosim.* **63**(2), 87-104 (1996).
17. A. Savitzky and M. Golay, *Smoothing and Differentiation of Data by Simplified Least Squares Procedures*, *Anal. Chem.* **36**, 1627-1639 (1964).
18. L.D. Hendrick and R.D. Edge, *Cosmic-Ray Neutrons Near the Earth*, *Phys. Rev.*, **145** (4), 1023-1025, (1965).
19. U.J. Schrewe, *Radiation Exposure Monitoring in Civil Aircraft*, *Nucl. Instr. and Meth. in Phys. Res. A*, **422**, 621-625 (1999).
20. M.J. McCall, *Development and Validation of a Predictive Code for AirCrew Radiation Exposure (PC-AIRE)*, M. Eng. Thesis, Royal Military College of Canada, April 2000.